SCIENCE CHINA
Physics, Mechanics & Astronomy

• Article •

August 2015 Vol. 58 No. 8: 084201
doi: 10.1007/s11433-015-5674-7

Selective excitation of resonances in gammadion metamaterials for terahertz wave manipulation†

WANG DaCheng, HUANG Qin, QIU ChengWei & HONG MingHui*

Department of Electrical and Computer Engineering, National University of Singapore, 4 Engineering Drive 3, 117581, Singapore

Received February 6, 2015; accepted March 12, 2015

A gammadion terahertz (THz) metamaterial embedded with a pair of splits is experimentally investigated. By introducing the pair of splits at different arms, the transmitted amplitude at the resonance frequency can be manipulated from 61% to 24%. Broadband static resonance tunability from 1.11 to 1.51 THz is also demonstrated via varying the relative split positions at certain arms. The amplitude change and static resonance tunability are attributed to the introduced split pairs, which enable selective excitation of different resonance modes in the gammadion metamaterials. This work promises a new approach to design THz functional devices.

terahertz, gammadion metamaterials, transmission

PACS number(s): 07.57.Pt, 42.25.Bs, 41.20.Jb, 78.20.Ci

Citation: Wang D C, Huang Q, Qiu C W, et al. Selective excitation of resonances in gammadion metamaterials for terahertz wave manipulation. Sci China-Phys Mech Astron, 2015, 58: 084201, doi: 10.1007/s11433-015-5674-7

1 Introduction

THz technology, a cutting edge research field, promises a family of wonderful applications, ranging from scanners in airport security, non-destructive inspection and quality control to bio-imaging, bio-sensing, high speed communication and astronomy [1]. All these intriguing applications are based on the unique properties of THz wave, which sits between microwaves and infrared radiation. For instance, THz wave can pass through many dielectric and semiconductor materials, but shows unique fingerprints when interacting with bio-molecules. Meanwhile, THz wave is a non-ionizing radiation, which is harmless to tissues for biological applications [2]. However, the interactions between THz wave and natural materials are weak, which limits the effective manipulation of THz wave. One of the promising approaches to push THz optics into real world applications is to manipulate THz wave based on artificial materials. In visible, infrared and microwave ranges, artificially designed materials have shown their uniqueness for novel optical properties, such as negative index [3], cloaking [4], extremely short wavelength [5–12] and strong dispersion [13–17]. These properties have led to revolutions in the entire field of subwavelength optics. Based on the extremely short wavelength of the collective excitation of electrons in metallic surfaces, Luo's group theoretically and experimentally demonstrated the deep-subwavelength interference effect in 2004 [5,7], which was further utilized to break Abbe's diffraction limit and achieve high-resolution optical imaging and lithography [8]. In 2005, Fang et al. [9] demonstrated that this sub-diffraction phenomenon was a direct consequence of the superlens effect. The extremely short wavelength of surface wave can also be utilized to modify traditional law of reflection and refraction [10]. Based on the revised law, a series of flat plasmonic devices were elaborately designed to realize functionalities such as abnormal beam deflection, subwavelength focusing and

*Corresponding author (email: elehmh@nus.edu.sg)
†Contributed by HONG MingHui (Associate Editor)

imaging [11,12]. Subsequently, other methods were proposed to achieve similar effects based on the phase shift induced in the process of polarization conversion [12]. Another important property of structured metamaterial is its strong dispersion [13]. Through proper dispersion engineering of anisotropic metamaterial, Luo's group presented the detailed theory and experimental validation of achromatic wave plates [14,15], which altered the classic Fresnel equations. At almost the same time, Grady et al. [16] also demonstrated similar results in the terahertz regime. Most recently, the dispersion of metasurface was successfully utilized to overcome the traditional thickness limit for perfect blackbody absorber [18]. Strikingly, it was shown that a 0.3 nm thick tungsten film can absorb almost all the microwave and even terahertz energy under coherent condition [17]. The above breakthroughs are critical to the design of THz metamaterials [19–23]. In recent years, researchers have studied various THz metamaterials to control the amplitude, phase, spatial propagation and polarization of THz wave [20–23]. Among the previous THz metamaterials, split ring resonators (SRRs) and gammadion structures are two widely investigated designs because they can effectively manipulate THz wave [24–31]. One of the limitations of SRR is that it only supports one fundamental resonance mode. This limitation can be eliminated in gammadion metamaterials because they support different resonance modes owing to the rotational symmetry. Previous work on gammadion metamaterials is mainly focused on stacking different layers of gammadion metamaterials and investigating the optical activities [29–31]. Little work has been done to study the different resonance modes in one layer of gammadion metamaterials, which may provide us a new freedom to manipulate THz wave based on these different resonance modes.

In this work, the design and experimental demonstration of a gammadion metamaterial structure embedded with a pair of splits is presented. By designing the split pair at different arms in the gammadion structure, we can achieve THz wave amplitude manipulation at the resonance frequency in the transmission spectra. Broadband static resonance tunability can also be realized by purposely changing the relative split positions at certain arms. The introduction of the splits provides us a novel approach to selectively excite different resonance modes in the gammadion metamaterials. The measured results are in good agreement with the numerical simulation. The gammadion metamaterial embedded with split pairs, as a simple and compact structure, can be applied to make efficient THz wave manipulation devices.

2 Structure design, fabrication and characterization

As shown in Figure 1(a), the original gammadion metamaterial structure has a side length of a = 60 μm and line width of w = 3 μm. The length of each arm is b = 30 μm. The whole pattern is periodic array of the basic unit in a square lattice with the periodicity of d = 100 μm. For illustration, the arms in this gammadion structure are labeled as A, B, C and D arms. This gammadion structure, different from conventional C shape SRR, has a four-fold degree of symmetry. In the gammadion structure, two components 1 and 2 shown in Figure 1(b) can be decomposed to investigate the resonance behaviors. Considering that the electric field of the incident THz wave is in the vertical direction, resonance intensity in component 1 is different from that in component 2. When a split pair is introduced at different arms, two components can be selectively excited to manipulate the incident THz wave. Figures 1(c) and (d) show the design of a split pair located in the middle of B and A arms with a split gap of 4 μm, which cut off one resonance component and only the other resonance component can be excited. Therefore, the amplitude of THz wave can be manipulated with respect to split positions at A and B arms. Figure 1(e) shows a split pair designed in C arm, which changes the resonance of component 1 and at the same time maintains the excitation of component 2. Thus, broadband static resonance tunability is realized by changing the relative positions of the split pair at C arm.

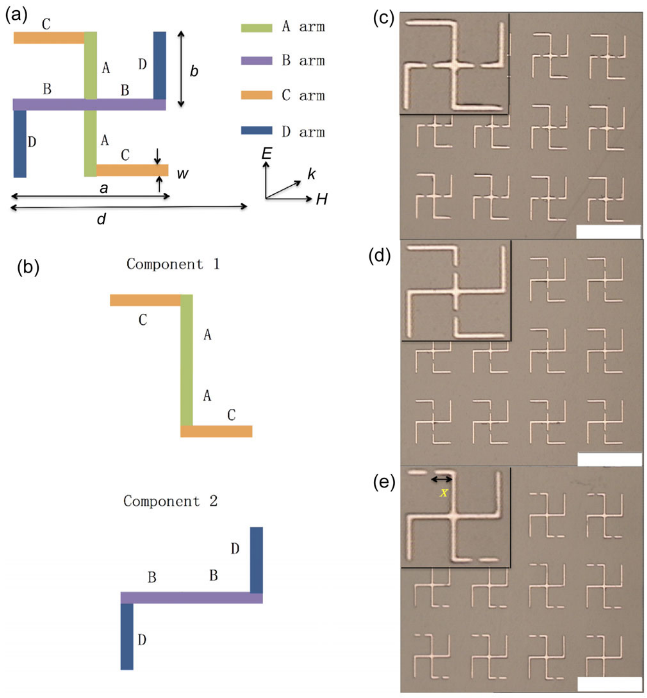

Figure 1 (Color online) (a) Schematic of the gammadion THz metamaterial structure. (b) Decomposition into two resonance components of the gammadion metamaterial structure. (c)–(e) The microscope images of the gammadion metamaterial structures embedded with split pairs in B, A and C arms, which were fabricated by laser MLA lithography. All the scale bars are 100 μm. The insets are metamaterial structure unit cells embedded with a split pair. The length x in (e) is the distance between the center of splits and A arm.

All the samples were fabricated by laser micro lens array (MLA) lithography on the 100 μm thick polyethylene naphthalate (PEN) films (Teonex Q51, Teijin Dupont Films) [32]. First, 1.5 μm thick positive photoresist S1813 was spin coated on the PEN film, followed by soft baking on a hotplate at 80°C for 60 s. The designed patterns were created on the photoresist by laser MLA lithography with UV light (λ= 355 nm) and more than 10000 unit cells of the designed patterns were fabricated on the substrate simultaneously. Then copper (Cu) thin film at the thickness of 200 nm was deposited onto the photoresist using an electron beam evaporator and followed by a lift-off processing to pattern the designed structures. The samples were measured by THz time domain spectroscopy (THz-TDS) system in transmission mode under a nitrogen environment to minimize water absorption. A bare PEN film was used as a reference sample and all the measured transmission spectra were normalized to the reference sample. Numerical simulation was carried out in commercial software CST Microwave Studio to simulate the transmission spectra, electric field distributions and surface current distributions at the resonance frequencies.

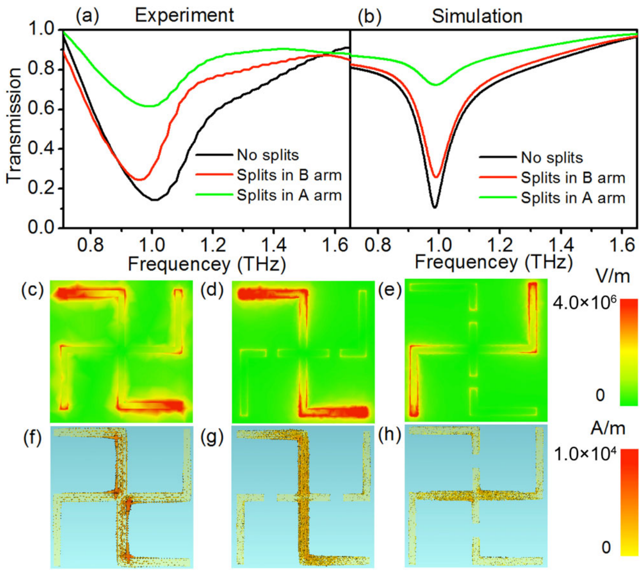

Figure 2 (Color online) (a) Measured and (b) simulated transmission spectra for the gammadion metamaterial structures without and with a split pair in B and A arms. (c)–(e) Simulated electric field distributions of the metamaterials without a split pair, with a split pair in B and A arms at 0.98 THz, respectively. The corresponding surface current distributions are shown in (f)–(h).

3 Results and discussion

3.1 Amplitude manipulation

The designed structures shown in Figures 1(c) and (d) were selected to investigate the THz wave amplitude manipulation. A split pair was introduced so as to maintain the rotational symmetry of the gammadion structure. The measured transmission spectra are shown in Figure 2(a). The gammadion metamaterial structure without the split pair presents a transmittance of 14% at the resonance frequency of 1.00 THz. When the split pair is introduced in the center of B arm, the transmittance becomes 24% at the resonance frequency of 0.97 THz. When two splits are designed in the middle of A arm, the transmission becomes 61% at the resonance frequency of 0.99 THz. The metamaterial without the split pair has the smallest transmission because both components 1 and 2 contribute to the resonance. When the split pair is embedded into different arms, components 1 and 2 can be selectively activated at different resonance intensities, which lead to different amplitudes of the transmitted THz wave at resonance frequencies. Figure 2(b) shows the simulated transmission spectra. It is observed that the metamaterial structure without a split pair shows the transmitted amplitude of 0.11 at 0.98 THz. When the splits are in the center of A and B arms, the amplitudes are 0.72 and 0.26 at 0.98 THz. The amplitude variation range for different split positions in the measured spectra is similar to the simulation data. The small difference between experimental and simulation results correspond to size variation during fabrication. The similar amplitude variation range indicates that such a new design can be applied to THz wave amplitude manipulation by selective excitation of the resonance components 1 and 2.

Figures 2(c)–(h) show the simulated electric field and surface current distributions of metamaterial structures without and with a split pair in B and A arms at the resonance frequencies. As shown in Figures 2(c) and (f), there are two major branches of current flow at the resonance frequency, which indicate that both components 1 and 2 contribute to the overall resonance behavior and the resonance is the strongest for this gammadion structure, resulting in the smallest transmission. As shown in Figures 2(d) and (g), when a split pair is introduced in the center of B arm, the current path for resonance component 2 is cut off by the split pair and only component 1 is excited. Therefore, the resonance intensity is small compared with the case without the split pairs, as only one component is responsible for this resonance behavior, which agrees well with the measured results. Figures 2(e) and (h) show the electric field and current distributions for the metamaterials with a split pair in the middle of A arms. In this case, only component 2 is active. However, as B arms in component 2 are normal to the polarization direction of the incident THz wave, the resonance intensity is not as strong as it in component 1. So the transmission amplitude in this metamaterial is larger than that with a split pair in B arms. Thus, by the introduction of a split pair in the gammadion metamaterials, two resonance modes can be selectively excited to modulate the amplitude of the transmitted THz wave from 61% to 23%. Note that these gammadion metamaterials embedded with a split pair have a rotational symmetry. In the case that the polarization of the incident electric field is fixed, the same piece of THz device can be used to manipulate THz wave at the resonance frequency by a simple rotation of 90°. Meanwhile, phase change materials, like VO_2, can be coupled into the split pair for active THz wave modulation [33]. To demonstrate the applicability of our design in active THz wave modulation, we simulated the transmission spectra when VO_2 was inserted into the splits in the design shown in Figure 1(d). In the simulation, the permittivity of VO_2 was set as $\varepsilon_r = 9$ and the conductivities σ were varied from 200 S/m to 4.4×10^5 S/m [34]. As shown in Figure 3, active amplitude modulation can be obtained from 0.71 to 0.41 at 0.96 THz with different conductivities of VO_2. Although the modulation range is slightly smaller than that without VO_2, such a design presents its applicability in THz optics, such as THz modulators and switches.

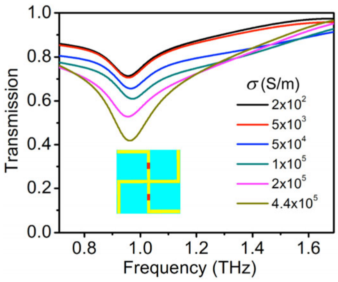

Figure 3 (Color online) Simulated transmission spectra of the gammadion metamaterials when VO_2 with different conductivities is embedded into the splits. The inserted image is the schematic of the design, in which the red part is the embedded VO_2.

3.2 Broadband static resonance frequency tunability

The metamaterial structure shown in Figure 1(e) was selected to study its broadband resonance frequency tunability by changing the relative positions of the split pair in C arm. When the distance x (shown in Figure 1(e)) between the center of the splits and A arm varies from 7 to 10, 13, 16, 19, 22 and 25 μm, the experimental results in Figure 4(a) show that the resonance frequency shifts from 1.51 to 1.44, 1.39, 1.30, 1.25, 1.18 and 1.11 THz, respectively. These resonances mainly attribute to component 1 due to the vertical polarization of incident THz wave. Component 2 presents a resonance at 1.01 THz for all the structures. This result is in agreement with the design shown in Figure 1(d) where only component 2 is excited at around 1.00 THz. But the amplitudes of the transmitted THz wave at 1.01 THz are different with respect to different relative distances x, which originate from different coupling intensities between components 1 and 2. When the distance x is 25 μm, the resonance frequency of component 1 is 1.11 THz, which is near the resonance frequency of component 2. Thus, these two resonances strongly couple with each other and form one broad resonance dip at 1.11 THz. When the distance x decreases, the resonance frequency of component 1 shifts to a higher frequency, which increases the difference of the resonance frequencies between components 1 and 2. Therefore, the coupling intensity between two resonances decreases. At the distance x of 7 μm, two resonance dips at 1.01 and 1.51 THz can be observed, which is attributed to the weak coupling of two resonances. Similar transmission spectra can be observed by the simulation in Figure 4(b). The similar variation trends in the transmission spectra suggest that by introducing

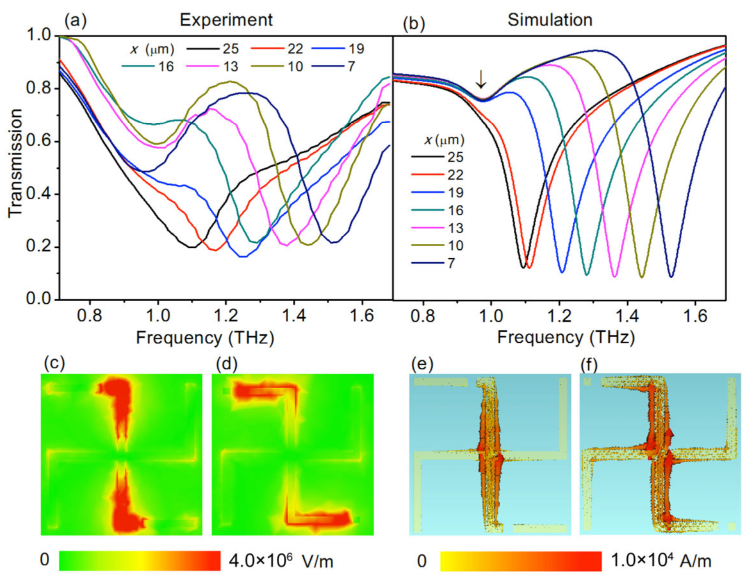

Figure 4 (Color online) (a) Measured and (b) simulated transmission spectra of the gammadion metamaterials with a split pair in C arm at a distance x of 7, 10, 13, 16, 19, 22 and 25 μm, respectively. (c) Simulated electric field distributions of the metamaterial structure with a split pair located at a distance x of 7 μm in C arm at 1.52 THz and its corresponding surface current distributions (e). (d) Simulated electric field distributions of the metamaterial structure with a split pair located at a distance x of 25 μm in C arm at 1.09 THz and its corresponding surface current distributions (f).

a split pair in C arm, we can change the resonance of component 1 and maintain the resonance of component 2. The coupling intensity between components 1 and 2 varies with respect to the relative distance x and leads to the broadband static resonance tunability property.

To further explore the resonance modes in these metamaterials, electric field distributions and surface current distributions at the resonance frequencies were simulated and shown in Figures 4(c)–(f). Figure 4(c) shows the electric field distributions of the metamaterials with a distance x of 7 μm at 1.52 THz and Figure 4(e) is its corresponding surface current distributions. It is clear that when a small part of component 1 is cut off by the split pair, the conducting path is shortened and the resonance frequency shifts to a higher frequency. In this case, component 1 resembles a bar and presents a dipole resonance at 1.52 THz. As this resonance frequency is far from the resonance frequency of component 2 at 0.98 THz, the coupling between components 1 and 2 is weak, which causes two dips to arise in the transmission spectra. When the distance x increases to 25 μm, the main conducting path of component 1 increases, leading to the decrease of the resonance frequency. Figure 4(d) shows the electric field distributions of the metamaterials with a distance x of 25 μm at 1.09 THz. It is observed that component 1 is mainly excited to contribute to the resonance at 1.05 THz, and component 2 is also excited to affect the overall resonance. As the resonance frequencies of components 1 and 2 are close to each other, the superposition between components 1 and 2 leads to a single broadband transmission dip at 1.09 THz. The surface current distribution at 1.09 THz in Figure 4(f) also confirms that component 1 is the main conducting path of the resonance and component 2 couples with component 1 to form one single transmission dip. Therefore, the relative positions of the split pair embedded in C arm selectively change the effective conducting path of component 1 and hence tune the resonance frequencies. The selective excitation of resonance modes with components 1 and 2 can be applied in the metamaterials to achieve broadband static resonance tunability, which extends the working frequency range in THz optics and has potential applications in functional broadband THz devices.

4 Conclusions

In summary, gammadion THz metamaterials embedded with a pair of splits for THz wave amplitude manipulation and broadband static resonance tunability have been demonstrated. By selectively exciting the desired resonance components in the gammadion metamaterials via introducing a split pair on different arms, the amplitude of the transmitted THz wave at the resonance frequency can be manipulated from 61% to 24%. The difference of the amplitudes is attributed to different resonance intensities of the two components in the gammadion metamaterials. Broadband static resonance tunability ranging from 1.11 THz to 1.51 THz can also be achieved through tuning the relative split pair positions at certain arms, which gives different coupling intensities between the two resonance components. This work promises a simple and efficient approach to construct new THz functional devices.

This work was supported by the National Research Foundation, Prime Minister's Office, Singapore under its Competitive Research Program (Grant No. NRF-CRP10-2012-04).

1 Tonouchi M. Cutting-edge terahertz technology. Nat Photon, 2007, 1: 97–105
2 Bykhovski A, Gelmont B. Influence of environment on terahertz spectra of biological molecules. J Phys Chem B, 2010, 114: 12349–12357
3 Smith D, Padilla W, Vier D, et al. Composite medium with simultaneously negative permeability and permittivity. Phys Rev Lett, 2000, 84: 4184–4187
4 Qiu C W, Hu L, Xu X F, et al. Spherical cloaking with homogeneous isotropic multilayered structures. Phys Rev E, 2009, 79: 047602
5 Luo X, Ishihara T. Subwavelength photolithography based on surface-plasmon polariton resonance. Opt Express, 2004, 12: 3055–3065
6 Hu C, Zhao Z, Chen X, et al. Realizing near-perfect absorption at visible frequencies. Opt Express, 2009, 17: 11039–11044
7 Luo X, Ishihara T. Surface plasmon resonant interference nanolithography technique. Appl Phys Lett, 2004, 84: 4780
8 Gao P, Yao N, Wang C, et al. Enhancing aspect profile of half-pitch 32 nm and 22 nm lithography with plasmonic cavity lens. Appl Phys Lett, 2015, 106: 093110
9 Fang N, Lee H, Sun C, et al. Sub-diffraction-limited optical imaging with a silver superlens. Science, 2005, 308: 534–537
10 Xu T, Wang C, Du C, et al. Plasmonic beam deflector. Opt Express, 2008, 16: 4753–4759
11 Xu T, Du C, Wang C, et al. Subwavelength imaging by metallic slab lens with nanoslits. Appl Phys Lett, 2007, 91: 201501
12 Yu N, Genevet P, Kats M A, et al. Light propagation with phase discontinuities: Generalized laws of reflection and refraction. Science, 2011, 334: 333–337
13 Feng Q, Pu M, Hu C, et al. Engineering the dispersion of metamaterial surface for broadband infrared absorption. Opt Lett, 2012, 37: 2133–2135
14 Pu M, Chen P, Wang Y, et al. Anisotropic meta-mirror for achromatic electromagnetic polarization manipulation. Appl Phys Lett, 2013, 102: 131906
15 Guo Y, Wang Y, Pu M, et al. Dispersion management of anisotropic metamirror for super-octave bandwidth polarization conversion. Sci Rep, 2015, 5: 8434
16 Grady N K, Heyes J E, Chowdhury D R, et al. Terahertz metamaterials for linear polarization conversion and anomalous refraction. Science, 2013, 340: 1304–1307
17 Pu M, Feng Q, Wang M, et al. Ultrathin broadband nearly perfect absorber with symmetrical coherent illumination. Opt Express, 2012, 20: 2246–2254
18 Rozanov K N. Ultimate thickness to bandwidth ratio of radar absorbers. IEEE Trans Antennas Propagat, 2000, 48: 1230–1234
19 Pu M, Wang M, Hu C, et al. Engineering heavily doped silicon for broadband absorber in the terahertz regime. Opt Express, 2012, 20: 25513–22519
20 Chen H T, Padilla W J, Cich M J, et al. A metamaterial solid-state

terahertz phase modulator. Nat Photonics, 2009, 3: 148–151
21 Wu J, Moser H O, Xu S, et al. From polarization-dependent to polarization-independent terahertz meta-foils. Appl Phys Lett, 2013, 103: 191114
22 Han J, Lakhtakia A, Qiu C W. Terahertz metamaterials with semiconductor split-ring resonators for magnetostatic tunability. Opt Express, 2008, 16: 14390–14396
23 Chen H T, Padilla W J, Zide J M O, et al. Active terahertz metamaterial devices. Nature, 2006, 444: 597–600
24 Singh R, Al-Naib I A I, Koch M, et al. Asymmetric planar terahertz metamaterials. Opt Express, 2010, 18: 13044–13050
25 Chen Z C, Hong M H, Lim C S, et al. Parallel laser microfabrication of large-area asymmetric split ring resonator metamaterials and its structural tuning for terahertz resonance. Appl Phys Lett, 2010, 96: 181101
26 Wang D, Qiu C, Hong M. Coupling effect of spiral-shaped terahertz metamaterials for tunable electromagnetic response. Appl Phys A, 2014, 115: 25–29
27 Chen Z C, Rahmani M, Gong Y D, et al. Realization of variable three dimensional terahertz metamaterial tubes for passive resonance tunability. Adv Mater, 2012, 24: Op143–Op147
28 Zhu Z H, Yang X, Gu J Q, et al. Broadband plasmon induced transparency in terahertz metamaterials. Nanotechnology, 2013, 24: 214003
29 Zhou J F, Chowdhury D R, Zhao R K, et al. Terahertz chiral metamaterials with giant and dynamically tunable optical activity. Phys Rev B, 2012, 86: 035448
30 Zhao R, Zhang L, Zhou J, et al. Conjugated gammadion chiral metamaterial with uniaxial optical activity and negative refractive index. Phys Rev B, 2011, 83: 035105
31 Kenanakis G, Zhao R, Katsarakis N, et al. Optically controllable THz chiral metamaterials. Opt Express, 2014, 22: 12149–12159
32 Han N R, Chen Z C, Lim C S, et al. Broadband multi-layer terahertz metamaterials fabrication and characterization on flexible substrates. Opt Express, 2011, 19: 6990–6998
33 Dicken M J, Aydin K, Pryce I M, et al. Frequency tunable near-infrared metamaterials based on VO_2 phase transition. Opt Express, 2009, 17: 18330–18339
34 Zhu Y H, Zhao Y, Holtz M, et al. Effect of substrate orientation on terahertz optical transmission through VO_2 thin films and application to functional antireflection coatings. J Opt Soc Am B, 2012, 29: 2373–2378